Inductive Voltage of Insert HTS Coils Due to Coil Deformation for Ultra-high Magnetic Field Generation

So Noguchi, Takanobu Mato, and Seungyong Hahn

***Abstract*—Some rare earth-barium-copper-oxide (REBCO) magnets have been developed as an "insert" to generate ultra-high magnetic fields in a bore of "outsert" background magnets, mainly owing to their good in-field capabilities to generate high fields. Meanwhile, REBCO ultra-high field magnets are known to have some technical challenges such as screening current-induced stress and the consequent plastic deformation that recently attracts much attention from magnet engineers. The coil geometry deformation not only causes mechanical damage to the REBCO layer but affects the screening current distribution itself. Significant coil deformation may lead to deformation of coil current, which results in additional inductive voltage change of individual coils having differential coil inductance. In this paper, we have investigated such extra inductive voltage due to coil configuration deformation using electromagnetic numerical simulation together with deformation finite element analysis. The simulation shows that an insert REBCO magnet for ultra-high magnetic field generation may have a small voltage rise induced by the coil inductance change. It also shows the screening current distribution change due to the coil deformation.**

***Index Terms*—Coil deformation, equivalent circuit model, HTS magnet, numerical simulation, screening current.**

I. Introduction

ULTRA-HIGH magnetic field (>30 T) generation has been under research and development in some institutes [1]–[4]. For generation of such high fields, rare earth-barium-copper-oxide (REBCO) magnets are known to be suitable as an "insert" in a bore of a background magnet, often named "outsert", due to superior in-field current carrying capacity and mechanical rigidity. Meanwhile, because of the thin flat shape of REBCO tape, large screening currents are induced in the REBCO layers, and magnetic fields are reduced [5]–[8]. Recently, techniques to reduce screening currents have attracted the attention from magnet engineers [9], [10], and the screening currents are simulated with various numerical methods as well [11]–[16]. In addition, it was recently pointed out that screening currents produced excessive hoop stresses, and plastic deformations occurred on one side edge of the REBCO tapes [17]. The behavior of screening current-induced fields also reveals the coil deformation [18]–[20]. These suggest that the insert REBCO magnet in a high magnetic field deforms, and such deformation affects the electromagnetic behaviors of the insert REBCO magnet.

We have previously developed the partial element equivalent circuit (PEEC) model to investigate screening current behaviors of REBCO pancake coils [21]. The model has been improved considering the effect of the coil configuration deformation [22]. Yet, the inductance change due to the deformation has been ignored mainly because it was expected to be negligible.

In recent years, we have been actively pursuing the generation of ultra-high magnetic fields, where we have observed higher voltages of an insert REBCO magnet under high fields than expected. We have investigated such extra voltage and now propose the inductance change as one of the key causes. The inductance change due to coil deformation has been simulated and the consequent extra voltage rise together.

II. Extra Voltage Term Due to Coil Deformation

Some insert REBCO pancake coils have been tested for ultra-high field generation [1]–[4], [23]. The electromagnetic behavior investigation of such insert REBCO pancake coils is indispensable for stable operation. Fig. 1 shows the equivalent circuit model of a no-insulation (NI) REBCO pancake coil, well-known as a "lumped" model [24], [25]. The following equation for the insert REBCO coil is obtained according to the second Kirchhoff's law:

$$V_{\mathrm{in}} + \frac{R_{\mathrm{SC}} R_{\mathrm{mt}}}{R_{\mathrm{SC}} + R_{\mathrm{mt}}} I_{\mathrm{in}} = R_{\mathrm{ct}} I_{\mathrm{ct}} \tag{1}$$

where V_{in}, R_{SC}, R_{mt}, I_{in}, R_{ct}, and I_{ct} are the inductive voltage of the NI REBCO coil, the REBCO layer resistance, the copper matrix resistance, the REBCO coil current in the azimuthal direction, the turn-to-turn contact resistance, and the REBCO coil current in the radial direction, respectively. Commonly, the

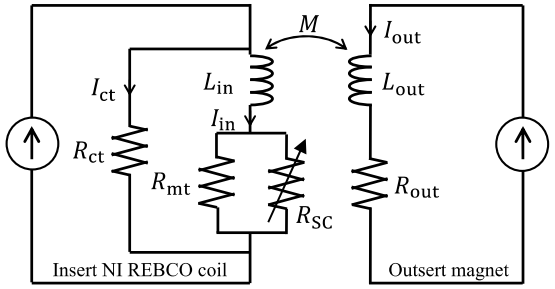

Fig. 1. Equivalent circuit model of ultra-high field magnet consisting of insert NI REBCO coils and an outsert magnet.

Manuscript received. This work was supported by the JSPS KAKENHI under Grant No. 20H02125. *(Corresponding author: So Noguchi.)*

S. Noguchi and T. Mato are with the Graduate School of Information Science and Technology, Hokkaido University, Sapporo 060-0814, Japan (e-mail: noguchi@ssi.ist.hokudai.ac.jp).

S. Hahn is with the Department of Electrical and Computer Engineering, Seoul National University, Seoul 08826, Korea (e-mail: hahnsy@snu.ac.kr).

inductive voltage is represented V_{in} by

$$V_{\text{in}} = L_{\text{in}} \frac{\mathrm{d}I_{\text{in}}}{\mathrm{d}t} + M \frac{\mathrm{d}I_{\text{out}}}{\mathrm{d}t} \quad (2)$$

where L_{in}, I_{out}, and M are, respectively, the self-inductance of insert NI REBCO coil, the current of the outset magnet, and the mutual inductance between insert and outsert magnets.

It has long been known that a large electromagnetic force causes the insert magnet to expand. Recently, the deformation of insert REBCO pancake coils for ultra-high magnetic field generation has been reported [18], [26], [27]. The insert REBCO coils deform greatly due to high current densities in high magnetic fields generated by the outsert magnets. Here, considering the inductance change due to the coil deformation, (2) must be revised to

$$V_{\text{in}} = N \frac{\mathrm{d}\Phi}{\mathrm{d}t} = L_{\text{in}} \frac{\mathrm{d}I_{\text{in}}}{\mathrm{d}t} + I_{\text{in}} \frac{\mathrm{d}L_{\text{in}}}{\mathrm{d}t} + M \frac{\mathrm{d}I_{\text{out}}}{\mathrm{d}t} + I_{\text{out}} \frac{\mathrm{dM}}{\mathrm{d}t} \quad (3)$$

$$N\Phi = L_{\text{in}} I_{\text{in}} + M I_{\text{out}} \quad (4)$$

where N and Φ are the number of turns of the REBCO coil and the flux through the REBCO coil. It is well known that when the coil deformation is small, the second and fourth terms of the right side on (3) can be ignored. Meanwhile, in the case of an ultra-high field magnet, since the outsert magnet generates a strong field with a high current, the fourth term of the right side on (3) cannot particularly be ignored to accurately simulate the electromagnetic behavior of insert NI REBCO pancake coils.

III. Simple Deformation Analysis

A. REBCO Coil Model and Charging Pattern

For the investigation of extra voltage rise due to coil deformation, we first simulated a simple NI REBCO double-pancake (DP) coils charging under 30 T generated by an outsert magnet. Table I lists the specifications of the NI REBCO DP coils, and Fig. 2(a) shows the illustration of the NI REBCO DP coils and the outsert magnet. Here, the NI REBCO DP coils are placed upwards by 100 mm. Fig. 2(b) shows the operating pattern: (1) the outsert magnet charges up to 30 T, and then (2) the NI REBCO DP coils charge up to 150 A with a ramp speed of 0.5 A/s and discharge to 0 A.

B. 1-D Deformation Simulation

In this model, the displacement analysis is conducted with one-dimensional (1-D) finite element method according to the following governing equations:

$$\frac{\partial \sigma_r}{\partial r} + \frac{\sigma_r - \sigma_\theta}{r} + JB_z = 0 \quad (5)$$

$$\varepsilon_r = \frac{1}{E_r}\sigma_r - \frac{\nu_{\theta r}}{E_\theta}\sigma_\theta$$
$$\varepsilon_\theta = -\frac{\nu_{r\theta}}{E_r}\sigma_r + \frac{1}{E_\theta}\sigma_\theta \quad (6)$$

$$\varepsilon_r = \frac{\partial u_r}{\partial r}$$
$$\varepsilon_\theta = \frac{u_r}{r} \quad (7)$$

where σ_r, σ_θ, J, and B_z are the radial and hoop stresses, the current density, and the axial magnetic field, respectively. ε_r, ε_θ, E_r, E_θ, ν_{12}, and u_r are the radial and hoop strains, and Young's moduli in the r and θ directions, the Poisson's ratio defined by $\nu_{12} = -\varepsilon_2/\varepsilon_1$, and the radial displacement in the radial direction.

According to the displacement of stress/strain simulation, the self- and mutual inductances are computed with Neumann formula [28] for deformed shapes of NI REBCO DP coils. Table II shows the parameters used for the deformation simulation. In this paper, all the material was supposed to be isotropic.

TABLE I
Specifications of 2 NI REBCO DP Coils

Number of DP coils	2
Number of turns per single pancake	23
Inner diameter; Outer diameter (mm)	32; 34
REBCO tape width (mm)	4.0
Total insert coil inductance (mH)	0.271
Field per current of DP coils (mT/A)	1.7
Operating temperature (K)	4.2

TABLE II
Mechanical Properties of Materials [20]

Young's moduli (GPa)	REBCO	178
	Hastelloy	200
	Copper	180
Poisson's ratio	REBCO	0.30
	Hastelloy	0.32
	Copper	0.35

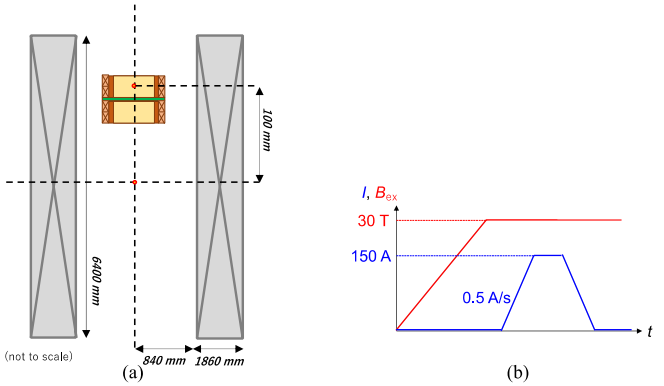

Fig. 2. (a) Illustration of cross section of insert NI REBCO DP coils and outsert magnet and (b) operating pattern: (1) charging outsert magnet to 30 T and (2) charging insert coils to 150 A with 0.5 A/s and then discharging to 0 A with the same ramp rate. The center of the upper DP coil was placed at 100 mm above the outsert magnet center.

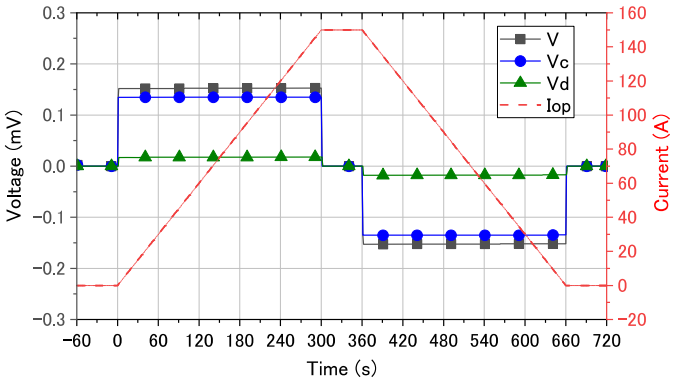

Fig. 3. Tme-transient coil voltage during charging and discharging the insert NI REBCO DP coils. V, Vc, Vd, and Iop are the total coil voltage (V = Vc + Vd), the normal inductive voltage, the inductive voltage due to coil deformation, and the operating current of NI REBCO DP coils, respectively.

C. Simulation Results

Fig. 3 shows the coil voltage with time during charging/discharging the insert REBCO DP coils. Here, the "normal inductive voltage" V_c is the voltage derived from the first and third terms of the right side on (3); i.e., it is the inductive voltage without considering the coil deformation. Since L_{in} = 0.271 mH and dI_{in}/dt = 0.5 A/s, the normal inductive voltage is 0.136 mV. The "inductive voltage due to coil deformation" V_d is generated by the second and fourth terms of the right side on (3). In the simulation, V_d is ~0.018 mV, ~13% of the normal inductive voltage V_c. The total inductive voltage V is the sum of V_c and V_d.

The insert NI REBCO DP coils keep expanding during charging, the small extra inductive voltage is induced by the coil inductance change. However, it might be hard to observe the extra inductive voltage of this level in measurement.

IV. More Complicated Simulation Method

In the previous simple model, the screening current is ignored, and it is supposed that the insert REBCO coils expand uniformly since the 1D FEM is employed. A few years ago, Kolb-Bond, *et al.* reported the REBCO tape rotation phenomenon [18], [29], [30]. In this chapter, the extra inductive voltage rise expressed with (3) is applied to the local deformation (REBCO tape rotation) of REBCO pancake coils.

A. Screening Current & Deformation Simulation Method

As a screening current simulation, an advanced partial element equivalent (APEEC) method proposed in [21] is employed. The two-dimensional (2-D) elastic FEM on *rz* plane is coupled with the APEEC to simulate the local plastic deformation, as shown in Fig. 4. The *BJR* stress distribution obtained from the APEEC simulation is used for the 2D elastic FEM as input data, and the displacement obtained from the 2D elastic FEM is employed for the APEEC simulation. In the APEEC, the inductance changes computed from the coil deformations are considered in the equivalent circuit like (3). The coil deformations are also used for the following computation of the equivalent resistance of REBCO layer, R_{SC}, according to the *J-B-θ* characteristics, where θ is the angle of the field to the tape surface, because the *c*-axis of REBCO layer is tilted from the radial direction:

$$R_{sc} = \frac{\ell}{A}\frac{E_c}{J}\left(\frac{J}{J_c(B,\theta)}\right)^n \tag{8}$$

where ℓ, A, E_c, J, J_c, B, and n are the length and area of REBCO tape, the electrical-field criteria (1 μV/cm), the current density, the critical current density, the magnetic field, and the power index, respectively. The coil deformation (REBCO tape rotation) corrects the magnetic field angle θ perpendicular to the wide REBCO tape surface. In this paper, it was assumed the *c*-axis orientation was identical to the direction perpendicular to the wide REBCO tape surface.

In the deformation simulation, the following governing equations are solved with the 2-D FEM:

$$\frac{\partial \sigma_r}{\partial r} + \frac{\partial \sigma_{rz}}{\partial z} + \frac{\sigma_r - \sigma_\theta}{r} + J_\theta B_z = \rho \frac{\partial^2 u_r}{\partial t^2} \tag{9}$$

$$\frac{\partial \sigma_{rz}}{\partial r} + \frac{\partial \sigma_z}{\partial z} + \frac{\sigma_{rz}}{r} - J_z B_r = \rho \frac{\partial^2 u_z}{\partial t^2}$$

$$\begin{aligned}
\varepsilon_r &= \frac{1}{E_r}\sigma_r - \frac{\nu_{\theta r}}{E_\theta}\sigma_\theta - \frac{\nu_{zr}}{E_z}\sigma_z \\
\varepsilon_\theta &= -\frac{\nu_{r\theta}}{E_r}\sigma_r + \frac{1}{E_\theta}\sigma_\theta - \frac{\nu_{z\theta}}{E_z}\sigma_z \\
\varepsilon_z &= -\frac{\nu_{rz}}{E_r}\sigma_r - \frac{\nu_{\theta z}}{E_\theta}\sigma_\theta + \frac{1}{E_z}\sigma_z
\end{aligned} \tag{10}$$

$$\begin{aligned}
\varepsilon_r &= \frac{\partial u_r}{\partial r} \\
\varepsilon_\theta &= \frac{u_r}{r} \\
\varepsilon_z &= \frac{\partial u_z}{\partial z}
\end{aligned} \tag{11}$$

where σ_{rz}, J_θ, J_z, B_r, ρ, u_z, ε_z, and E_z are the shear stress, the current density in the azimuthal and axial directions, the radial field, the mass density, the axial displacement, the axial strain, and Young's module in the *z* direction, respectively.

B. Simulation Results

Table III lists the specifications for a simulated insert REBCO pancake coil having an outsert magnet of 31.1 T. This insert REBCO pancake coil is also placed upwards by 250 mm. As an operating pattern, (1) the outsert magnet is energized up to 31.1 T, (2) the insert REBCO coil charges to 400 A twice, and then (3) the outsert magnet is deenergized (see the top graph of Fig. 6). Fig. 6 also shows the deformed coil shapes with current density distributions. At the coil current I_{op} = 400 A, the upper edge of REBCO coil largely deforms; i.e., the self-

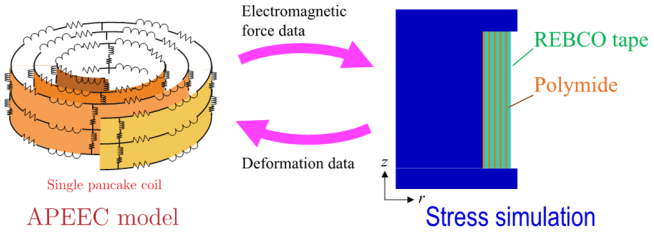

Fig. 4. Screening current APEEC simulation and FEM stress simulation are alternatively conducted.

TABLE III
Specifications of Insert REBCO Single Pancake Coils

Number of pancake coils	1
Number of turns per single pancake	5
Inner diameter (mm)	120
REBCO tape width (mm)	4.0
Operating temperature (K)	4.2

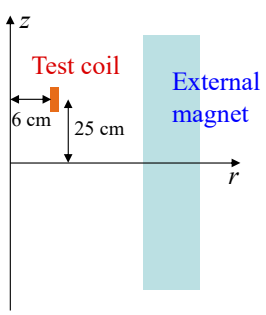

Fig. 5. Illustration of cross section of insert REBCO coil and outsert magnet.

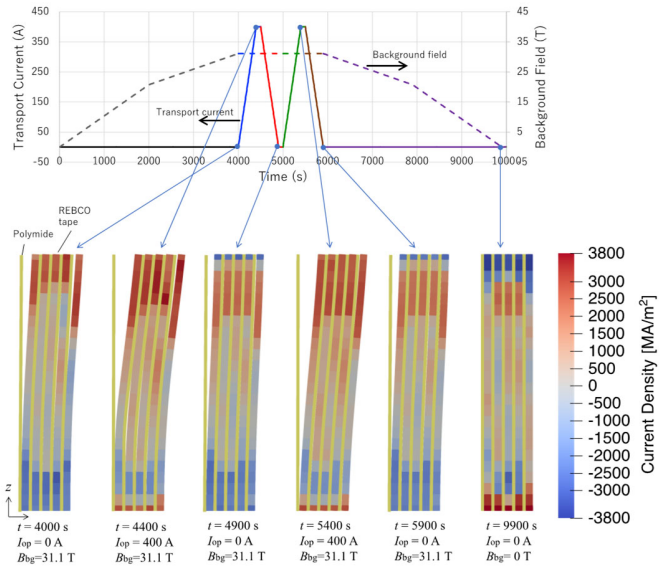

Fig. 6. (Top) Operation patter. (Bottom) current distribution map on deformed shape of 5-turn REBCO coil.

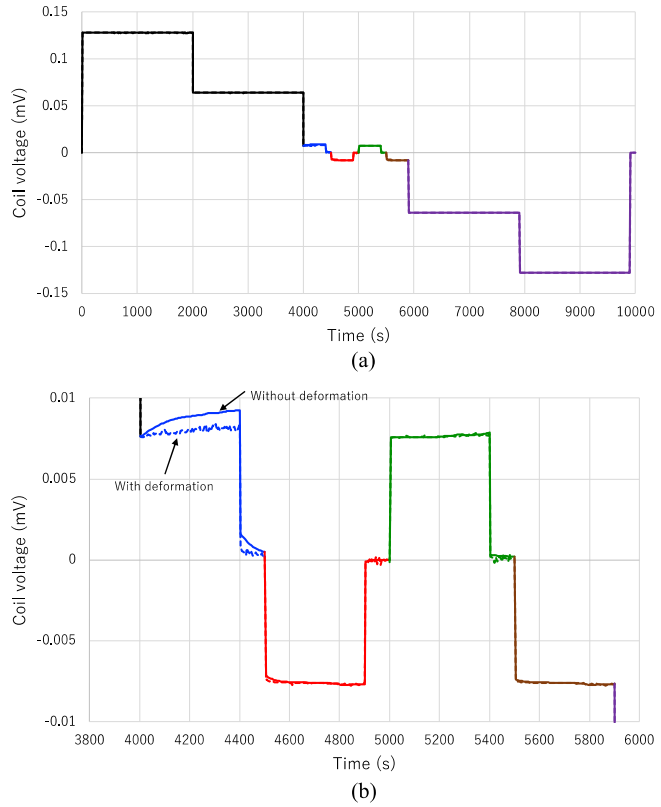

Fig. 7. (a) induced coil voltage and (b) enlarged view during charging/discharging insert REBCO coil. The line color corresponds to the operation patter in Fig. 6(a).

/mutual inductances also change.

Fig. 7(a) shows the REBCO coil voltage with time. When charging/discharging the outsert magnet, the high voltage is induced in the insert REBCO coil, whereas no current flows. Fig. 7(b) gives the enlarged graph during the insert REBCO coil charging/discharging, where the dotted and solid lines mean the voltage with/without coil deformation effect, respectively.

At the first charging of the REBCO pancake coil, the voltage of the deformed coil (the blue dotted line in Fig. 7) is smaller than that of the non-deformed coil (the blue solid line). As mentioned in [18], the screening current is reduced by the REBCO tape rotation. Although the inductive voltage rises by the coil deformation, the coil voltage is more reduced by the REBCO tape rotation. Since the insert REBCO coil inductance is 7.73 μH, the ideal coil voltage is 7.73 μV (= 7.73 μH × 1 A/s). Meanwhile, the phenomenon that REBCO coil voltage rises due to the screening current was presented in [31]; however, in the experiment, the REBCO coil was not deformed because of very small *BJR* stress without external magnetic field. Here, the *BJR* stress is derived from the multiplication of the magnetic field, the current density, and the radius. The peak stress and field in the REBCO tape are 746 MPa and 7.2 T, respectively.

At the first and second discharging and the second charging, no large difference can be seen. These screening current distribution is different from that of the first charging.

As the result, the upper part of REBCO coil is largely expanded by the screening current effect; on contrast, the lower part is not deformed. Unlike the first simulation case in this paper, since the REBCO coil is not expanded on whole, the extra voltage rise caused by the coil expansion cannot be seen. We will keep investigating the extra voltage rise for various insert REBCO pancake coils.

V. Conclusion

In this paper, an extra inductive voltage generated by the coil inductance change is investigated in simulation. Recently, it was reported that mechanical deformation may cause the critical current density degradation and the screening current distribution change. Furthermore, since the flux penetrating into insert REBCO coils changes, the self-/mutual inductances also change. In particular, an insert REBCO coil operating in high current density under ultra-high magnetic fields may expand mechanically. And such expansion may induce an extra voltage rise in the insert REBCO coil. The screening current is then substantially affected by the extra voltage rise due to the change of self-/mutual inductance values.

References

[1] S. Hahn, *et al.*, "45.5-tesla direct-current magnetic field generated with a high-temperature superconducting magnet," *Nature*, vol. 570, pp. 496-499, Jun. 2019.

[2] W. D. Markiewicz, *et al.*, "Design of a superconducting 32 T magnet with REBCO high field coils," *IEEE Trans. Appl. Supercond.*, vol. 22, no. 3, Jun. 2012, Art. no. 4300704.

[3] Y. Iwasa, *et al.*, "A high-resolution 1.3-GHz/54-mm LTS/HTS NMR magnet," *IEEE Trans. Appl. Supercond.*, vol. 25, no. 3, Jun. 2015, Art. no. 4300205.

[4] J. Liu, *et al.*, "World record 32.25 tesla direc-current magnetic field generated with an all-superconducting magnet," *Supercond. Sci. Technol.*, vol. 33, no. 3, Feb. 2020, Art. no. 03LT01.

[5] H. Miyazaki, S. Iwai, T. Uto, Y. Otani, M. Tkahashi, T. Tosaka, K. Tasaki, S. Nomura, T. Kurusu, H. Ueda, S. Noguchi, A. Ishiyama, S. Urayama, and H. Fukuyama, "Screening-current-induced magnetic field of conduction-cooled HTS magnets wound with REBCO-coated conductors," *IEEE Trans. Appl. Supercond.*, vol. 27, no. 4, Jun. 2017, Art. no. 4701705.

[6] D. Uglietti, Y. Yanagisawa, H. Maeda, and T. Kiyoshi, "Measurements of magnetic field induced by screening currents in YBCO solenoid coils," *Supercond. Sci. Technol.*, vol. 23, Sep. 2010, Art. no. 115002.
[7] G. Dilasser, P. Fazilleau, and P. Tixador, "Experimental measurement and numerical simulation of the screening current-induced field decay in a small ReBCO coil," *IEEE Trans. Appl. Supercond.*, vol. 27, no. 4, Dec. 2017, Art. no. 4900104.
[8] H. Ueda, M. Fukuda, K. Hatanaka, T. Wang, A. Ishiyama, and S. Noguchi, "Spatial and temporal behavior of magnetic field distribution due to shielding current in HTS coil for cyclotron application," *IEEE Trans. Appl. Supercond.*, vol. 23, no. 3, Jun. 2013, Art. no. 4100805.
[9] K. Kajikawa and Y. Okabe, "Reduction of screening-current-induced fields in an HTS tape winding using toroidal arrangement of shaking coil," *IEEE Trans. Appl. Supercond.*, vol. 26, no. 4, Jun. 2016, Art. no. 4400504.
[10] H. Miyazaki, *et al.*, "Screening-current-induced magnetic field of conduction-cooled HTS magnets wound with REBCO-coated conductors," *IEEE Trans. Appl. Supercond.*, vol. 27, no. 4, Jun. 2017, Art. no. 4701705.
[11] R. Itoh, Y. Oga, S. Noguchi, H. Igarashi, and H. Ueda, "Numerical simulation of screening current distribution in HTS tape of high field magnet," *Physica C*, vol. 484, pp. 300–304, Jan. 2013.
[12] H. Ueda, J. Saito, Y. Ariya, A. Mochida, T. Wang, X. Wang, K. Agatsuma, and A. Ishiyama, "Reduction of irregular magnetic field generated by screening current in REBCO coil," *IEEE Trans. Appl. Supercond.* Vol. 25, no. 3, Jun. 2015, Art. no. 6603205.
[13] S. Noguchi, S. Hahn, H. Ueda, S. Kim, and A. Ishiyama, "An extended thin approximation method to simulate screening current induced in REBCO coils," *IEEE Trans. Magn.*, vol. 54, no. 3, Mar. 2018, Art. no. 7201904.
[14] T. Mifune, N. Tominaga, Y. Sogabe, Y. Mizobata, M. Yasunaga, A. Ida, T. Iwashita, and N. Amemiya, "Large-scale electromagnetic field analyses of coils wound with coated conductors using a current-vector-potential formulation with a thin-strip approximation," *Supercond. Sci. Technol.*, vol. 32, no. 9, Jul. 2019, Art. no. 094002.
[15] S. Noguchi, T. Imai, D. Park, S. Hahn, and Y. Iwasa, "A simple screening current simulation method using equivalent circuit model for REBCO pancake coils," *Supercond. Sci. Technol.*, vol. 33, no. 11, Sep. 2020, Art. no. 115005.
[16] E. Berrospe-Juarez, V. M. R. Zermoño, F. Trillaud, and F. Grilli, "Real-time simulation of large-scale HTS systems: multi-scale and models using the *T-A* formulation," *Suerpcond. Sci. Technol.*, vol. 32, no. 6, Apr. 2019, Art. no. 065003.
[17] S. Hahn, K. L. Kim, K. Kim, K. Bhattarai, K. Radcliff, X. Hu, T. Painter, I. Dixon, and D. Larbalestier, "Progress in No-Insulation HTS Magnet Researches," *presented at Applied Superconductivity Conference 2018*.
[18] D. Kolb-Bond, M. Bird, I. R. Dixon, and T. Painter, "Screening current rotation effects: SCIF and strain in REBCO magnets," *Supercond. Sci. Technol.*, vol. 34, no. 9, Sep. 2021, Art. no. 095004.
[19] Y. Yan, Y. Li, and T. Qu, "Screening current induced field and stress in ultra-high-field magnets using REBCO coated conductors," *Supercond. Sci. Technol.*, vol. 35, no. 1, Dec. 2021, Art. no. 014003.
[20] H. Ueda, H. Maeda, Y. Suetomi, and Y. Yanagisawa, "Experiment and numerical simulation of the combined effect of winding cool-down, and screening current induced stresses in REBCO coils," *Supercond. Sci. Technol.*, vol. 35, no. 5, Mar. 2022, Art. no. 054001.
[21] S. Noguchi and S. Hahn, "A newly developed screening current simulation method for REBCO pancake coils based on extension of PEEC model," *Supercond. Sci. Technol.*, vol. 35, no. 4, Mar. 2022, Art. no. 044005.
[22] S. Noguchi, T. Mato, K. Kim, and S. Hahn, "Electromagnetic Behavior Simulation of REBCO Pancake Coils Considering REBCO Tape Rotation Under High Magnetic Field," submitted for publication.
[23] J. B. Song, X. Chaud, B. Borgnic, F. Debray, P. Fazilleau, and T. Lécrevisse, "Construction and test of a 7 T metal-as-insulation HTS insert under a 20 T high background magnetic field at 4.2 K," *IEEE Trans. Appl. Supercond.*, vol. 29, no. 5, Aug. 2019, Art. no. 4601705.
[24] S. Hahn, D. K. Park, J. Bascuñán, and Y. Iwasa, "HTS pancake coils without turn-to-turn insulation," *IEEE Trans. Appl. Supercond.*, vol. 21, no. 3, pp. 1592-1595, Jun. 2011.
[25] X. Wang, S. Hahn, Y. Kim, J. Bascuñán, J. Voccio, H. Lee, and Y. Iwasa, "Turn-to-turn contact characteristics for an equivalent circuit model of no-insulation ReBCO pancake coil," *Supercond. Sci. Technol.*, vol. 26, no. 3, Mar. 2013, Art. no. 035012.
[26] X. Hu, *et al.*, "Analyses of the plastic deformation of coated conductors deconstructed from ultra-high field test coils," *Supercond. Sci. Technol.*, vol. 33, no. 9, Jul. 2020, Art. no. 095012.
[27] T. Mato and S. Noguchi, "Plastic deformation simulation of REBCO tapes using particle methods," *IEEE Trans. Appl. Supercond.*, vol. 32, no. 6, Sep. 2022, Art. no. 8400705.
[28] S. Noguchi, "Electromagnetic, thermal, and mechanical quench simulation of NI REBCO pancake coils for high magnetic field generation," *IEEE Trans. Appl. Supercond.*, vol. 29, no. 5, Aug. 2019, Art. no. 4602607.
[29] Y. Li, D. Park, W. Lee, Y. Choi, H. Tanaka, J. Bascuñán, and Y. Iwasa, "Screening-current-induced strain gradient on REBCO conductor: an experimental and analytical study with small coils wound with monofilament and striated multifilament REBCO tapes," *IEEE Trans. Appl. Supercond.*, vol. 30, no. 4, Feb. 2020, Art. no. 4702305.
[30] Y. Yan, P. Song, C. Xin, M. Guan, Y. Li, H. Liu, and T. Qu, "Screening-current-induced mechanical strains in REBCO insert coils," *Supercond. Sci. Technol.*, vol. 34, Jun. 2021, Art. no. 085012.
[31] J. Lee, "A study on the equivalent circuit analysis of no-insulation and metal-insulation HTS coils considering the turn-to-turn capacitance and conductance," presented at ASC 2022, Hawaii, 2LPo2A-08, Oct. 2022.